PHYSICAL REVIEW B **93**, 041415(R) (2016)

Measurement of the Zak phase of photonic bands through the interface states of a metasurface/photonic crystal

Qiang Wang,[1] Meng Xiao,[2] Hui Liu,[1,*] Shining Zhu,[1] and C. T. Chan[2]

[1]*National Laboratory of Solid State Microstructures, School of Physics, Collaborative Innovation Center of Advanced Microstructures, Nanjing University, Nanjing 210093, China*

[2]*Department of Physics, Institute for Advanced Study, the Hong Kong University of Science and Technology, Clear Water Bay, Kowloon, Hong Kong*

(Received 21 May 2015; revised manuscript received 24 December 2015; published 21 January 2016)

The Zak phase labels the topological property of one-dimensional Bloch bands. Here we propose a scheme and experimentally measure the Zak phase in a photonic system. The Zak phase of a bulk band is related to the topological properties of the two band gaps sandwiching this band, which in turn can be inferred from the existence or absence of an interface state. Using a reflection spectrum measurement, we determined the existence of interface states in the gaps and then obtained the Zak phases. The knowledge of Zak phases can also help us predict the existence of interface states between a metasurface and a photonic crystal. By manipulating the property of the metasurface, we can further tune the excitation frequency and the polarization of the interface state.

DOI: 10.1103/PhysRevB.93.041415

Topological invariance plays a more and more important role in modern physics with the discovery of new materials, such as topological insulators [1,2]. The concept of momentum space topology has also been extended to various photonic systems [3–16] to realize interesting applications. In a two-dimensional system, the topological invariant is characterized by the first Chern number [17,18], which is proportional to the Berry phase [19] enclosing the first Brillouin zone. In a one-dimensional (1D) system [20,21], the topological invariant can be characterized by the Zak phase [22], a special kind of Berry phase defined along a 1D bulk band.

One of the major challenges about the topological invariant is how to measure it, which is quite difficult as it is an abstract concept and hence hard to be observed directly. In recent years, topological invariants have been measured in cold atom systems [23–25] and an acoustic system [26]. A few methods have also been proposed to measure topological invariants in electromagnetic wave systems [27–33]. Recently, Xiao *et al.* theoretically investigated the relationship between the Zak phases and the surface impendence in 1D photonic crystals (PCs) [34]. Inspired by this work, here we propose a method and experimentally measure the Zak phases through interface states.

The schematic of our system is illustrated in Fig. 1(a), which is composed of a metal film (or metasurface) and a PC. A detailed structure is given in Fig. 1(b). A unit cell is composed of $A/B/A$ layers as marked by the red dashed lines in Fig. 1(b). Here, layer A is HfO_2 with a thickness of $t_a = 177.6$ nm and layer B is SiO_2 with a thickness of $t_B = 579.8$ nm. The unit length is $\Lambda = 2t_A + t_B = 935$ nm. We calculate its band dispersion as shown in Fig. 2(a) which covers the range of $1.1 < \Lambda/\lambda < 1.9$, including two bands (third and fourth bands counting from low frequency to high frequency) and three gaps (second, third, and fourth gaps). The refractive indexes of HfO_2 and SiO_2 used are from experimental measurements [35]. In the working frequency range, the dispersion is negligible, and the refractive indexes of HfO_2 and SiO_2 are around 2 and 1.46, respectively. The Zak phase is defined as [22]

$$\theta_n^{\mathrm{Zak}} = \int_{-\pi/\Lambda}^{\pi/\Lambda} \left[i \int_{\text{unit cell}} dz\, \varepsilon(z) u_{n,q}^*(z) \partial_q u_{n,q}(z) \right] dq, \quad (1)$$

where $\varepsilon(z)$ is the relative permittivity and $u_{n,q}$ is the normalized periodic part of the electric-field Bloch eigenfunction of a state on the nth band with wave vector q. As the value of the Zak phase depends on the choice of origin [36], here we choose it to be the interface of the two-layer A, which is also the boundary of the unit cell. The values of the Zak phases of bands 3 and 4 are calculated and labeled in green in Fig. 2(a), which are 0 for band 3 and π for band 4.

Besides Eq. (1), we can also determine the Zak phase using the symmetry of the band edge states. As the unit cell possesses mirror symmetry, the band edge states are either even or odd with respect to the mirror plane. Here, the symmetry types of the band edge states are defined using the symmetry of the eigenelectric field (see the Supplemental Material [37]). The symmetries of the six band edge states are labeled with red (symmetric) and blue (antisymmetric) circles, respectively, in Fig. 2(a). If the two band edge states of the same band have the same symmetry, the Zak phase of this band is 0, otherwise, the Zak phase is π [22,38]. However, the determination of the symmetry types of the band edge states is quite difficult to implement experimentally in optical frequency.

According to the surface bulk correspondence [34], the Zak phase is related to the signs of the reflection phases, i.e.,

$$\exp\left(i\theta_n^{\mathrm{Zak}}\right) = -\mathrm{sgn}(\varphi_n)/\mathrm{sgn}(\varphi_{n-1}), \quad (2)$$

where θ_n^{Zak} is the Zak phase of the nth bulk band, φ_{n-1} and φ_n are the reflection phases of the $(n-1)$th gap (gap blow the nth bulk band) and nth gap (gap above the nth bulk band), respectively. Measuring the value of the reflection phase inside a band gap may need a complex interference experimental setup [39]. However, Eq. (2) shows that we only need the sign, which greatly simplifies the measurement.

*Corresponding author: liuhui@nju.edu.cn

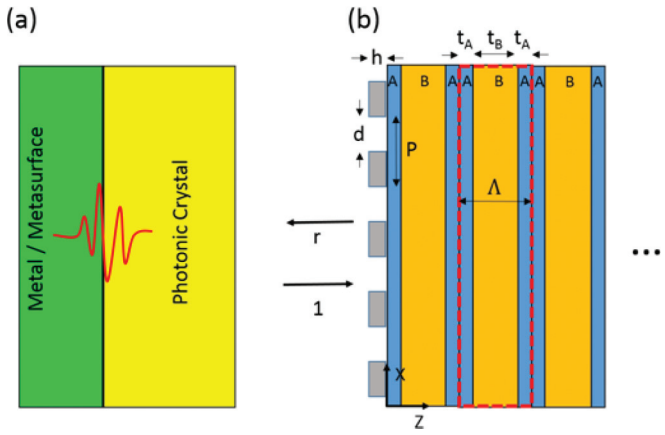

FIG. 1. (a) Sketch of an interface between a metal film (or metasurface) and a photonic crystal which supports interface states. (b) Sketch of the metasurface/photonic crystal system. The metasurface consists of nanoslits etched on a silver film with width d, period P, and thickness h. The period of the photonic crystal is Λ with $A/B/A$ as its unit cell as marked by the red dashed lines. Here, layer A is HfO_2, and layer B is SiO_2.

As the two band edge states sandwiching a gap must possess different symmetry types as required by the orthogonality, there are only two combinations: The first combination is a symmetric lower band edge state and an antisymmetric higher band edge state, which is denoted as S-A, for instance, gaps 3 and 4. The other is an antisymmetric lower band edge state and a symmetric higher band edge state (A-S), for example, gap 2. The difference between these two combinations is manifested in their reflection phase range [34]. For S-A-type gaps, the

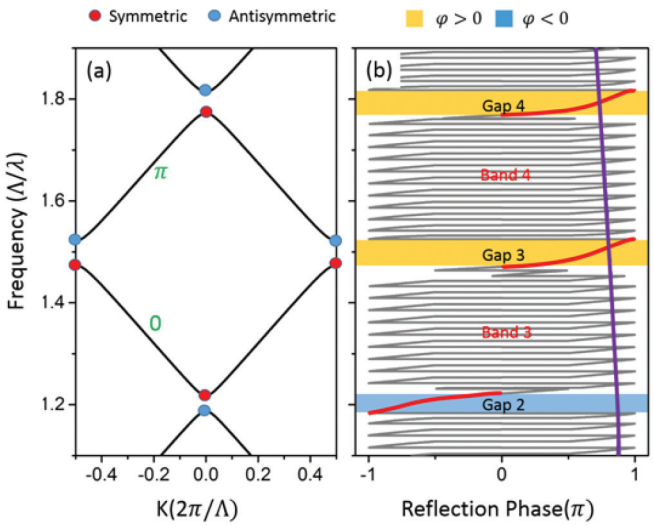

FIG. 2. (a) The band structure of the PC shown in Fig. 1(b) with $t_A = 177.6$ and $t_B = 579.8$ nm. The Zak phases are labeled in green. (b) The gray curves represent the reflection phase (φ_{PC}) of the 1D PC consisting of 12 periods. The reflection phases inside the gap regions are highlighted in red. The yellow (blue) region represents the gap with reflection phase $\varphi_{PC} > 0$ ($\varphi_{PC} < 0$). The purple line shows the negative value of the reflection phase ($-\varphi_{Ag}$) of a 70-nm-thick silver film.

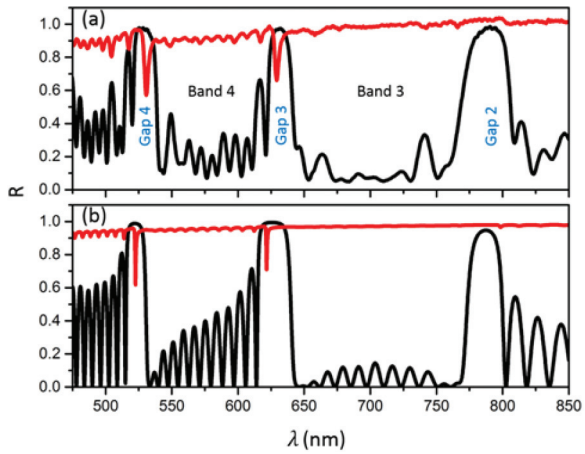

FIG. 3. (a) Experimental and (b) numerical reflection spectra of the PC (black line) and the silver film/PC (red line). The sharp dips of the red curve inside the gap frequency regions of the PC represent interface states between the silver film and the PC.

reflection phase belongs to $(0,\pi)$ and that of the A-S type belongs to $(-\pi,0)$, similar to a metal of which the sign of the reflection phase is also negative. Note that the reflection phase inside a band-gap region of a 1D PC does not change sign [34]. We numerically calculate the reflection phase (φ_{PC}) in gray as shown in Fig. 2(b). The reflection phases inside the gap regions are highlighted in red. The reflection phases of gaps 3 and 4 are positive and highlighted with a yellow color, whereas that of gap 2 is negative and is highlighted in blue. In experiment, we fabricated one PC sample according to the design in Fig. 1(b) with the same parameters as used in Fig. 2. The sample includes 12 periods ($A/B/A$). We measured the reflection spectrum of the sample, and the result is shown as the black curve in Fig. 3(a), which matches well with the numerical simulation shown as the black curve in Fig. 3(b).

The Tamm plasmon state [40,41] can be constructed in the system if we deposit a silver film on the PC. In experiment, the thickness of the silver film is 70 nm. The negative value of its reflection phase ($-\varphi_{Ag}$) is numerically calculated and shown in Fig. 2(b) with purple lines. The existence condition of an interface state is governed by the equation $\varphi_{PC} + \varphi_{Ag} = 0$. And hence if there is an interface state inside a gap region, we know the sgn(φ_{PC}) inside this gap must be positive. Otherwise, sgn(φ_{PC}) is negative. The crossing points in band gaps 3 and 4 satisfy $\varphi_{PC} + \varphi_{Ag} = 0$, which indicate the existence of an interface state. As a comparison, there is no crossing point in band gap 2, which means no interface state inside gap 2. According to the discussion above, Eq. (2) can be rewritten as

$$\theta_n^{\mathrm{Zak}} = \begin{cases} 0, & V_{n-1} \neq V_n, \\ \pi, & V_{n-1} = V_n, \end{cases} \tag{3}$$

where V_{n-1} and V_n indicate whether there exists an interface state or not in the lower and upper gaps, respectively, of the nth band. If the nth gap possesses interface states, $V_n = 1$, otherwise, $V_n = 0$. Equation (3) means, if the two adjacent band gaps possess or do not possess interface states simultaneously, the Zak phase of that band takes value π, otherwise, it takes 0. Experimentally, the existence of an interface state can be seen from the reflection spectrum which

TABLE I. The symmetry of band edge states, the reflection phase range of band gaps, and the Zak phases of bulk bands. The yellow (blue) regions represent the existence (the absence) of an interface state inside this gap.

Gap 2	Zak phase of Band 3	Gap 3	Zak phase of Band 4	Gap 4
A-S $\{-\pi, 0\}$	0	S-A $\{0, \pi\}$	π	S-A $\{0, \pi\}$

is presented as a dip inside the gap region. In Fig. 3(a), the red curve shows the reflection spectrum measured with normal incidence. The two sharp dips in gap 3 and gap 4 indicate the existence of interface states ($V_{3,4} = 1$), whereas there is no interface state in band gap 2 ($V_2 = 0$), and the corresponding results are summarized in Table I where yellow (blue) means there exists (does not exist) an interface state inside this gap. Besides a little global shift, which we think stems from the difference between the refractive index of materials in the experiments and those in the theoretical model, all the results match well with the numerical simulations in Fig. 3(b). According to Eq. (3), we can obtain the values of the Zak phase of band 3 as $\theta_3^{\text{Zak}} = 0$ and band 4 as $\theta_4^{\text{Zak}} = \pi$.

In the above investigation, the interface state is localized at the boundary between a silver film and a PC, whose frequency is determined by the structural parameters of the PC and the silver film. Different from the zero-energy edge states protected by the chiral symmetry [42], the interface state here is protected by the inherent mirror symmetry of the PC. To predict the existence of an interface state, we do not need to identify any topological transitional points [43,44], instead we only need the topological properties of the gaps on both sides of the interface to be different, which are related to the summation of the Zak phases of all the bulk bands below this gap [34]. We note that in crystalline topological insulators [45], the edge termination must be compatible with the symmetry used to define the bulk topology in order to guarantee bulk-edge correspondence. In our system, the edge termination must be at mirror planes in order for the bulk-edge correspondence to predict the existence of edge modes.

In applications, it is highly desirable that the working frequency can be tuned without changing the PC structure, and this can be achieved by replacing the metal film with a metasurface. Metasurfaces, which are composed of optical metamaterials in a reduced dimensionality, are applied to many novel interesting applications [46–63]. If we replace the silver film with metasurfaces, the interface state in the metasurface/PC configuration can be manipulated through engineering the reflection phase of the metasurface. Our metasurface possesses strong anisotropy and is designed to be composed of a subwavelength grating and a thin Si_3N_4 film. With this metasurface, we are able to manipulate both the excitation frequency and the polarization of the interface states.

The structure of our metasurface/PC configuration is shown schematically in Fig. 1(b). The structure parameters of the PC are $t_A = 97.5$ and $t_B = 267.0$ nm. The metasurface is composed of a subwavelength silver grating and a thin Si_3N_4 film. The slits in the grating are etched from a 50-nm-thick

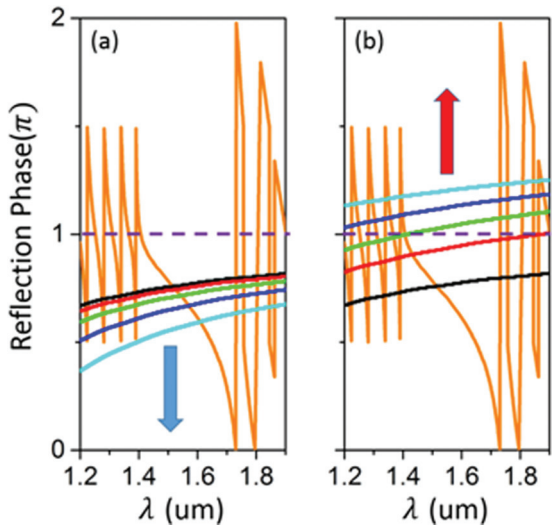

FIG. 4. The calculated negative value of the reflection phase of the metasurfaces (including the 55-nm-thick Si_3N_4 film) with (a) the Y polarization and (b) the X polarization. The black, red, green, blue, and cyan lines represent slit widths $d = 0$ (equivalent to the silver film), 50, 100, 150, and 200 nm, respectively. The orange line shows the reflection phase of the PC with $t_A = 97.5$ and $t_B = 267.0$ nm. The number of periods of the photonic crystal is 16.

silver film by a focused ion beam (FIB), whose width can be precisely controlled in the process. Between the PC and the grating, we insert a 55-nm-thick (much less than the working wavelength at about 1.5μm) Si_3N_4 film by plasma-enhanced chemical-vapor deposition, which protects the surface of the PC from being damaged by FIB. The nanoslits are periodical along the X direction with a thickness of $h = 50$ nm and a period of $P = 300$ nm. The width of a single slit is d, which is a tunable parameter in experiments. We fabricate five samples with different slit widths $d = 0$ (equivalent to a silver film), 50, 100, 150, and 200 nm. The calculated negative value of the reflection phases of the metasurfaces with the Y polarization (electric along the Y direction) and the X polarization (electric along the X direction) are shown in Figs. 4(a) and 4(b), respectively. The black, red, green, blue, and cyan lines represent the silt widths $d = 0$, 50, 100, 150, and 200 nm, respectively. For reference, the calculated reflection phase and the measured reflection spectrum of our PC are also shown in Figs. 4 and 5 as orange lines. Comparing Fig. 4(a) with 4(b), the reflection phases of the Y and the X polarizations have the opposite trends with the increasing of d (denoted by arrows in Fig. 4). Due to the reflection phase change in the metasurface, the crossing points inside the gap region shift accordingly, and hence interface states with different polarizations will shift in different directions. For the Y polarization, the curve of the metasurface shifts downward with increasing d (denoted by the blue arrow) and always has a crossing point with the curve of the PC in the gap region. However, for the X polarization, the curve of the metasurface shifts upward (denoted by the red arrow), and when $d > 100$ nm, there is no crossing point and hence no interface state. The different responses of different polarizations lie in the fact that the metasurface is highly anisotropic. It behaves like a metal slab for the Y

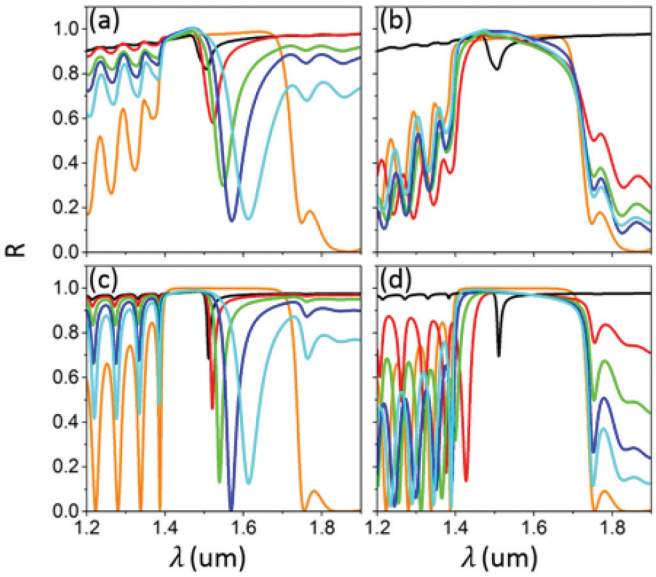

FIG. 5. Reflection spectrum of the metasurface/PC shown in Fig. 1(b) with (a) and (c) the Y polarization and (b) and (d) the X polarization where a, b, and (c,d) are the experimental (numerical) results. The black, red, green, blue, and cyan lines represent slit widths $d = 0$ (equivalent to the silver film), 50, 100, 150, and 200 nm, respectively. The orange line represents the reflection spectrum of the PC.

polarization and a dielectric slab for the X polarization. For the Y polarization, the existence of an interface state is protected, and we can only shift the frequency of the interface state inside the band gap.

The above results can also be seen from the reflection spectrum, which is measured by Fourier transformation infrared spectroscopy with normal incidence. The measured data are shown in Fig. 5(a) for the Y polarization and in Fig. 5(b) for the X polarization, respectively. The sharp dips inside the band gap on the reflection spectra indicate the existences of interface states. In Fig. 5(a), the frequency of the dip is redshifted with the increasing values of d. Consistent with the absence of crossing inside the gap region in Fig. 4(b) for the $d = 100$ nm, 150 nm, and 200 nm cases, we cannot find reflection dips for those three cases. The dip of the $d = 50$ nm case gets a little mixed up with the bulk band Fabry-Pérot crinkle as it is near the band edge and the PC is finite in the experiment. As a comparison, we also present the numerical results in Figs. 5(c) and 5(d) for the Y and the X polarizations, respectively. The numerical and experimental results match well with each other. Our results demonstrated the polarization selection of the interface states using the metasurface/PC configurations.

Due to the large field intensity enhancement, the interface state can be used in those applications which require large local fields, such as controlling the spontaneous optical emission from quantum dots [64], realizing a single photon source [65], and demonstrating nanolasers [66,67]. In addition, the meta-superstructure at the photonic crystal surface can be designed to manipulate the interface state for applications, such as optical switches [68] and sensors [69].

To summarize, we implemented an experiment to measure the Zak phases in a layered optical system. Instead of probing the reflection phase or the symmetry of band edge states, we determined the Zak phase through the interface state, which is indicated in the reflection spectrum. Although our focus here is on a one-dimensional system, this method can be extended to 2D or 3D systems. Besides, we showed the manipulation of interface states including both the excitation frequency and the polarization by introducing metasurfaces. The flexible control of the interface states at the boundary of the metasurface/PC is an area that deserves more investigation and may lead to new applications.

This work was financially supported by the National Natural Science Foundation of China (Grants No. 11321063, No. 61425018, and No. 11374151), the National Key Projects for Basic Researches of China (Grants No. 2012CB933501 and No. 2012CB921500), the Hong Kong Research Grant Council Grant No. AoE/P-02/12, the SRFDP/RGC ERG Joint Research Scheme Grant No. M-HKUST601/12, the Doctoral Program of Higher Education (Grant No. 20120091140005), and the Dengfeng Project B of Nanjing University.

Q. Wang and M. Xiao contributed equally to this work.

[1] M. Z. Hasan and C. L. Kane, Rev. Mod. Phys. **82**, 3045 (2010).
[2] X.-L. Qi and S. -C. Zhang, Rev. Mod. Phys. **83**, 1057 (2011).
[3] F. D. M. Haldane and S. Raghu, Phys. Rev. Lett. **100**, 013904 (2008).
[4] Z. Wang, Y. D. Chong, J. D. Joannopoulos, and M. Soljacic, Phys. Rev. Lett. **100**, 013905 (2008).
[5] Z. Wang, Y. D. Chong, J. D. Joannopoulos, and M. Soljacic, Nature (London) **461**, 772 (2009).
[6] Y. E. Kraus, Y. Lahini, Z. Ringel, M. Verbin, and O. Zilberberg, Phys. Rev. Lett. **109**, 106402 (2012).
[7] M. Hafezi, E. A. Demler, M. D. Lukin, and J. M. Taylor, Nat. Phys. **7**, 907 (2011).
[8] K. J. Fang, Z. F. Yu, and S. H. Fan, Nat. Photon. **6**, 782 (2012).
[9] M. C. Rechtsman, J. M. Zeuner, Y. Plotnik, Y. Lumer, D. Podolsky, F. Dreisow, S. Nolte, M. Segev, and A. Szameit, Nature (London) **496**, 196 (2013).
[10] A. B. Khanikaev, S. H. Mousavi, W. K. Tse, M. Kargarian, A. H. MacDonald, and G. Shvets, Nat. Mater. **12**, 233 (2013).
[11] M. C. Rechtsman, J. M. Zeuner, A. Tunnermann, S. Nolte, M. Segev, and A. Szameit, Nat. Photon. **7**, 153 (2013).
[12] L. Lu, L. Fu, J. D. Joannopoulos, and M. Soljacic, Nat. Photon. **7**, 294 (2013).
[13] M. Hafezi, S. Mittal, J. Fan, A. Migdall, and J. M. Taylor, Nat. Photon. **7**, 1001 (2013).
[14] L. Lu, J. D. Joannopoulos, and M. Soljaclc, Nat. Photon. **8**, 821 (2014).
[15] W. J. Chen, S. J. Jiang, X. D. Chen, B. C. Zhu, L. Zhou, J. W. Dong, and C. T. Chan, Nat. Commun. **5**, 5782 (2014).

[16] W. Tan, Y. Sun, H. Chen, and S. Q. Shen, Sci. Rep. **4**, 3842 (2014).
[17] D. J. Thouless, M. Kohmoto, M. P. Nightingale, and M. den Nijs, Phys. Rev. Lett. **49**, 405 (1982).
[18] D. Xiao, M. C. Chang, and Q. Niu, Rev. Mod. Phys. **82**, 1959 (2010).
[19] M. V. Berry, Proc. R. Soc. London, Ser. A **392**, 45 (1984).
[20] C. W. Ling, M. Xiao, C. T. Chan, S. F. Yu, and K. H. Fung, Opt. Express **23**, 2021 (2015).
[21] C. Poli, M. Bellec, U. Kuhl, F. Mortessagne, and H. Schomerus, Nat. Commun. **6**, 6710 (2015).
[22] J. Zak, Phys. Rev. Lett. **62**, 2747 (1989).
[23] M. Atala, M. Aidelsburger, J. T. Barreiro, D. Abanin, T. Kitagawa, E. Demler, and I. Bloch, Nat. Phys. **9**, 795 (2013).
[24] M. Aidelsburger, M. Lohse, C. Schweizer, M. Atala, J. T. Barreiro, S. Nascimbene, N. R. Cooper, I. Bloch, and N. Goldman, Nat. Phys. **11**, 162 (2015).
[25] L. Duca, T. Li, M. Reitter, I. Bloch, M. Schleier-Smith, and U. Schneider, Science **347**, 288 (2015).
[26] M. Xiao, G. C. Ma, Z. Y. Yang, P. Sheng, Z. Q. Zhang, and C. T. Chan, Nat. Phys. **11**, 240 (2015).
[27] S. Longhi, Opt. Lett. **38**, 3716 (2013).
[28] J. M. Zeuner, M. C. Rechtsman, Y. Plotnik, Y. Lumer, S. Nolte, M. S. Rudner, M. Segev, and A. Szameit, Phys. Rev. Lett. **115**, 040402 (2015).
[29] M. Hafezi, Phys. Rev. Lett. **112**, 210405 (2014).
[30] C. E. Bardyn, S. D. Huber, and O. Zilberberg, New J. Phys. **16**, 123013 (2014).
[31] W. C. Hu, J. C. Pillay, K. Wu, M. Pasek, P. P. Shum, and Y. D. Chong, Phys. Rev. X **5**, 011012 (2015).
[32] A. V. Poshakinskiy, A. N. Poddubny, and M. Hafezi, Phys. Rev. A **91**, 043830 (2015).
[33] W. S. Gao, M. Xiao, C. T. Chan, and W. Y. Tam, Opt. Lett. **40**, 5259 (2015).
[34] M. Xiao, Z. Q. Zhang, and C. T. Chan, Phys. Rev. X **4**, 021017 (2014).
[35] http://refractiveindex.info.
[36] R. Resta, Rev. Mod. Phys. **66**, 899 (1994).
[37] See Supplemental Material at http://link.aps.org/supplemental/10.1103/PhysRevB.93.041415 for the symmetry types of the band edges of PC1 and PC2. The simulation reflection phase of metasurfaces are presented. Besides, the E fields distribution of the interface states are provided.
[38] W. Kohn, Phys. Rev. **115**, 809 (1959).
[39] B. J. Vakoc, S. H. Yun, J. F. de Boer, G. J. Tearney, and B. E. Bouma, Opt. Express **13**, 5483 (2005).
[40] M. Kaliteevski, I. Iorsh, S. Brand, R. A. Abram, J. M. Chamberlain, A. V. Kavokin, and I. A. Shelykh, Phys. Rev. B **76**, 165415 (2007).
[41] K. Leosson *et al.*, Opt. Lett. **37**, 4026 (2012).
[42] S. Ryu and Y. Hatsugai, Phys. Rev. Lett. **89**, 077002 (2002).
[43] N. Malkova, I. Hromada, X. Wang, G. Bryant, and Z. Chen, Opt. Lett. **34**, 1633 (2009).
[44] M. C. Rechtsman, Y. Plotnik, J. M. Zeuner, D. Song, Z. Chen, A. Szameit, and M. Segev, Phys. Rev. Lett. **111**, 103901 (2013).
[45] L. Fu, Phys. Rev. Lett. **106**, 106802 (2011).
[46] N. F. Yu, P. Genevet, M. A. Kats, F. Aieta, J. P. Tetienne, F. Capasso, and Z. Gaburro, Science **334**, 333 (2011).
[47] X. Ni, N. K. Emani, A. V. Kildishev, A. Boltasseva, and V. M. Shalaev, Science **335**, 427 (2012).
[48] A. Pors, O. Albrektsen, I. P. Radko, and S. I. Bozhevolnyi, Sci. Rep. **3**, 2155 (2013).
[49] Y. Zhao and A. Alù, Phys. Rev. B **84**, 205428 (2011).
[50] X. B. Yin, Z. L. Ye, J. Rho, Y. Wang, and X. Zhang, Science **339**, 1405 (2013).
[51] G. Li, M. Kang, S. Chen, S. Zhang, E. Y.-B. Pun, K. W. Cheah, and J. Li, Nano Lett. **13**, 4148 (2013).
[52] N. K. Grady, J. E. Heyes, D. R. Chowdhury, Y. Zeng, M. T. Reiten, A. K. Azad, A. J. Taylor, D. A. R. Dalvit, and H.-T. Chen, Science **340**, 1304 (2013).
[53] C. Pfeiffer, C. Zhang, V. Ray, L. J. Guo, and A. Grbic, Phys. Rev. Lett. **113**, 023902 (2014).
[54] X. Cai, J. Wang, M. J. Strain, B. Johnson-Morris, J. Zhu, M. Sorel, J. L. O'Brien, M. G. Thompson, and S. Yu, Science **338**, 363 (2012).
[55] S. Sun, Q. He, S. Xiao, Q. Xu, X. Li, and L. Zhou, Nat. Mater. **11**, 426 (2012).
[56] N. Shitrit, I. Yulevich, E. Maguid, D. Ozeri, D. Veksler, V. Kleiner, and E. Hasman, Science **340**, 724 (2013).
[57] O. Y. Yermakov, A. I. Ovcharenko, M. Song, A. A. Bogdanov, I. V. Iorsh, and Y. S. Kivshar, Phys. Rev. B **91**, 235423 (2015).
[58] L. L. Huang *et al.*, Nat. Commun. **4**, 2808 (2013).
[59] W. T. Chen *et al.*, Nano Lett. **14**, 225 (2014).
[60] M. Esfandyarpour, E. C. Garnett, Y. Cui, M. D. McGehee, and M. L. Brongersma, Nat. Nanotechnol. **9**, 542 (2014).
[61] V. S. Asadchy, Y. Ra'di, J. Vehmas, and S. A. Tretyakov, Phys. Rev. Lett. **114**, 095503 (2015).
[62] L. Zhang, T. Koschny, and C. M. Soukoulis, Phys. Rev. B **87**, 045101 (2013).
[63] M. Decker, C. Kremers, A. Minovich, I. Staude, A. E. Miroshnichenko, D. Chigrin, D. N. Neshev, C. Jagadish, and Y. S. Kivshar, Opt. Express **21**, 8879 (2013).
[64] O. Gazzano, S. M. de Vasconcellos, K. Gauthron, C. Symonds, J. Bloch, P. Voisin, J. Bellessa, A. Lemaître, and P. Senellart, Phys. Rev. Lett. **107**, 247402 (2011).
[65] O. Gazzano, S. M. de Vasconcellos, K. Gauthron, C. Symonds, P. Voisin, J. Bellessa, A. Lemaître, and P. Senellart, Appl. Phys. Lett. **100**, 232111 (2012).
[66] C. Symonds, A. Lemaître, P. Senellart, M. H. Jomaa, S. Aberra Guebrou, E. Homeyer, G. Brucoli, and J. Bellessa, Appl. Phys. Lett. **100**, 121122 (2012).
[67] C. Symonds, G. Lheureux, J. P. Hugonin, J. J. Greffet, J. Laverdant, G. Brucoli, A. Lemaître, P. Senellart, and J. Bellessa, Nano Lett. **13**, 3179 (2013).
[68] W. L. Zhang and S. F. Yu, Opt. Commun. **283**, 2622 (2010).
[69] F. Giorgis, E. Descrovi, C. Summonte, L. Dominici, and F. Michelotti, Opt. Express **18**, 8087 (2010).